Available online at www.sciencedirect.com
SCIENCE DIRECT®
International Journal of Heat and Mass Transfer 47 (2004) 5271–5283
International Journal of HEAT and MASS TRANSFER
www.elsevier.com/locate/ijhmt

Base to apex thermal conductance of a cone embedded in a non-ideal insulator

William F. Pickard *

Department of Electrical and Systems Engineering, Washington University, Saint Louis, MO 63130, USA

Received 22 December 2003; received in revised form 11 June 2004

Abstract

As a paradigm for the effective thermal conductivity of a densely packed dispersion of conducting filler particles in an insulating matrix, the effective conductance of a cubic array of quasi-bicones is determined analytically and its numerical properties investigated. Based upon the insights gained, the effective conductivities of simple cubic arrays of more general particles are predicted by three different approximate techniques, and the results compared with those known for simple cubic arrays of spheres.

Keywords: Cone; Composite; Constitutive parameters; Homogenization of two-phase systems; Iterative embedding; Thermal boundary resistance

1. Introduction

In modern electronics, there is considerable interest in conveniently applied pastes which can be deposited upon electronic assemblies to increase locally either (i) the effective permittivity (dielectric constant) or (ii) the thermal conductivity. Such pastes typically consist of an electrically insulating organic matrix of low permittivity ($\varepsilon_m/\varepsilon_0 \lesssim 4$) and/or low thermal conductivity ($\kappa_m \lesssim 1\ \mathrm{W\,K^{-1}\,m^{-1}}$) within which have been suspended dispersant-coated electrically insulating filler particles of much higher permittivity ($\varepsilon_f/\varepsilon_0 \gtrsim 100$) and/or ($\kappa_f \gtrsim 20\ \mathrm{W\,K^{-1}\,m^{-1}}$). For both permittivity and thermal conductivity there is a large literature, both experimental and theoretical, which agrees on the following:

(i) Densely packing the packing low-constitutive-parameter matrices with high-constitutive-parameter fillers does *not* yield mixtures whose effective constitutive parameters closely approach those of the fillers. Rather it yields mixtures whose parameters typically are only 10-fold those of their matrices.
(ii) Particulate fillers which approximate flat plates of mixed size yield parameter increases which can be several-fold better than those of filler particles which approximate spheres of uniform size (e.g. [1]).

Extensive details can be found in a variety of pertinent review articles [2–7]. However, a first-order understanding of the phenomenon can be simply acquired from an elementary model for permittivity (a demonstration for thermal conductivity is substantially analogous and will be treated in the following sections).

* Tel.: +1 314 935 6104; fax: +1 314 935 7500.
E-mail address: wfp@ese.wustl.edu.

0017-9310/$ - see front matter © 2004 Elsevier Ltd. All rights reserved.
doi:10.1016/j.ijheatmasstransfer.2004.06.021

Nomenclature

Latin symbols

a	in Fig. 1D, the radius of a small perfectly-conducting hemisphere
A	a constant defined in Eq. (5)
$\mathscr{A}(\rho)$	a function defined in Eq. (42)
${}_k\mathfrak{A}_v$	angular eigenfunctions defined by Eqs. (11) and (19)
b	radius of a sphere in which an analytically tractable model will be solved. $b = s\sqrt{2}$
B	a constant defined in Eq. (5)
C	a capacitance, sometimes subscripted
d	the thickness of a surface layer of a filler particle and within which the Kapitza resistance is localized
$f\left(\frac{z}{s}\right)$	in Section 4, the normalized radius ρ of a filler particle
$F_{\mathrm{f}}\left(\frac{z}{s}\right)$	in a particle of filler, the total downward heat flux across a z-plane
${}_2F_1(\ldots)$	the ordinary hypergeometric function
${}_kF_v$	a system of constants
$\mathscr{F}$	at a surface, the inward directed flux density
${}_kG_v$	a system of constants
$\mathscr{G}$	a thermal conductance
${}_kH_v$	a system of constants
$\mathbf{I}_k$	a system of constants defined by Eq. (24a)
K, L	constants defined in Eq. (46)
P_v	a Legendre function of the first kind
r	for a cylindrical or spherical coordinate system, the radial coordinate
R	the lumped resistance of a thin spatial element
${}_k\mathscr{R}_v$	a radial eigenfunction defined by Eqs. (11), (15), (18)
s	radius of sphere of filler material
T	temperature
T_0	filler temperature at ($\theta = 0$; $r = b$)
$\mathbf{W}_{kk}$	a system of constants defined by Eq. (24b)
z	for a cylindrical coordinate system, the axial coordinate

Greek symbols

β	$\beta = \kappa_{\mathrm{f}}/\kappa_{\mathrm{m}} - 1$
γ	a positive exponent
δ	$\delta = d/s$
ε	permittivity
ε_0	permittivity of free space
ζ	the dimensionless axial coordinate z/s
$\zeta_{\min}$	a dimensionless constant given by $(d/s)(\kappa_{\mathrm{m}}/\kappa_{\mathrm{i}}) + (\kappa_{\mathrm{m}}/\kappa_{\mathrm{f}})\frac{1}{1+\Omega}$
η_k	a system of constants defined by Eq. (17′)
θ	polar angle of a spherical geometry
θ_0	polar angle of the cone in Fig. 1D
κ	thermal conductivity
Λ	$\ln(b/a)$
ξ	an exponent such that $0 < \xi \leqq 1$
ρ	the dimensionless radial coordinate r/s
υ	for a heterogeneous two phase mixture, the volume fraction of filler
ϕ	azimuthal angle of a cylindrical or spherical coordinate geometry (normally taken as possessing a right-handed screw sense with respect to the z-axis)
Φ	functions defined by Eqs. (7), (8), (20)
χ	$\cos\theta$
ω	a constant defined in Eq. (42)
Ω	the fan out factor of current entering a filler particle near its apex

Hebrew symbol

$\overline{\mathsf{P}}_v(\chi)$	a second solution of Legendre's equation and equal to $P_v(-\chi)$

Subscripts

eff	indicates and effective quantity (usually refers to a two component heterogeneous mixture)
f	filler material
i	interfacial material
m	matrix material
norm	indicates a normalized quantity
μ	for real eigendegrees, a real variable in the interval $(-1, 1)$ defined as $v = -\frac{1}{2} + \frac{1}{2}\mu$
v	complex degree of a Legendre function: $v = \sigma + \mathrm{i}\tau$ frequently used as shorthand for v_k, the kth eigendegree
σ	real part of the complex degree of a Legendre function
τ	imaginary part of the complex degree of a Legendre function

Superscript

*	indicates that the variable is constrained to a specific surface

Consider a cubical volume, s [m] on a side, containing a heterogeneous mixture of two immiscible components, matrix and filler; and suppose that the volume fraction of filler is denoted υ. Let these two components then be separated into layers of thickness υs for the filler and $(1 - \upsilon)s$ for the matrix. Because capacitances in series sum harmonically

$$\frac{1}{C_{\text{eff}}} = \frac{1}{C_{\text{f}}} + \frac{1}{C_{\text{m}}}; \tag{1a}$$

or, using the classic approximation for parallel-plate capacitors

$$\frac{1}{\varepsilon_{\text{eff}}} = \frac{\upsilon}{\varepsilon_{\text{f}}} + \frac{1-\upsilon}{\varepsilon_{\text{m}}}, \tag{1b}$$

and

$$\frac{\varepsilon_{\text{eff}}}{\varepsilon_{\text{f}}} = \frac{[\varepsilon_{\text{m}}/\varepsilon_{\text{f}}]}{1-\upsilon+\upsilon[\varepsilon_{\text{m}}/\varepsilon_{\text{f}}]}. \tag{1c}$$

Eq. (1c) reveals what experimentalists have qualitatively found to be the case for systems of this type: that mixing constituents of $[\varepsilon_{\text{m}}/\varepsilon_{\text{f}}] \ll 1$ to make a paste for which the effective constitutive parameter closely approaches ε_{f} is a formidable task since it requires a volume fraction υ so close to 1 as to be unattainable by simple random packing of granular particles!

The physics, unlike the detailed mathematics, of this behavior of this are as straightforward as the simple theory put forth above. The filler, being low impedance, captures the flux. But the filler is discontinuous so that, from time to time, this flux must "portage" across a layer of the relatively more insulating matrix material. This is beautifully illustrated in Fletcher's review of a decade ago [8, Fig. 2; cf. 9; p. 630] [1] which shows two rough surfaces in apposition and sketches the concentration of flux lines at points of contact. Ideally, the surfaces of two apposed filler particles make contact only at a small number of points, adjacent to which the flux is forced out into the intervening matrix. Thus the matrix dominates.

For heat conduction, the situation can be further complicated by the fact that both filler and matrix are often required to be electrically insulating so that heat conduction is by way of phonon propagation. Suitable dielectric crystals can have surprisingly high thermal conductivity, which however is disrupted at filler–matrix interfaces leading to the phenomenon of thermal boundary resistance [9–11].

The difficult task of understanding a particular constitutive parameter for a composite has been complicated by the history of this field. Recognizing the analytic difficulties of solving a microscale problem, workers have sensibly focussed on macroscale models which do not directly exploit the equation of heat conduction to evaluate the thermal behavior near a *point* of tangency between two filler particles. This issue will be directly confronted in the Sections 2 and 3 by evaluating exactly the thermal conductance of a modified cone-plane geometry. Section 4 will then be devoted to developing three easy approximate techniques for treating filler particles of more complicated non-conical shapes; and the approximation results for a cone will then be compared with the exact result.

[1] Where appropriate, pointers will be given to page (p.), section (s.), chapter (ch.), equation (Eq.), figure (Fig.), table (Tab.), or experiment (expt.) of the pertinent reference.

2. Development of the model

In this, as in many exercises in applied mathematics, success depends heavily upon setting the problem in such a way that it becomes analytically tractable without losing its relevance to the presumed physical situation. A composite of heterogeneous filler particles in a matrix will not in general possess the type of periodic structure which would simplify a mathematical model. Neither, however, will the structure be totally random; and an attractive idealization is a simple cubic lattice formed by files of identical spheres and their surrounding matrix, of which a *yz*-cross-section is shown in Fig. 1A. Each vertical *z*-directed file constitutes a conductance in parallel with each other vertical file and (since it is indistinguishable) can be considered as an independent entity; this has been indicated in Fig. 1A by patterning the spheres of one file. Similarly, if there are U spheres in one vertical file, then the file can be decomposed into 2U mathematically identical half-cells, which (by symmetry) will be idealized as bounded at top and bottom by isothermal (alternatively, equiflux) planes (black) and on the sides by insulating planes (dashed black), and it will be symmetric about its central axis; one such half-cell has been indicated in Fig. 1A by boxing it.

To proceed to the next level of simplification it is necessary to assume that κ_{f} [$\text{W K}^{-1}\text{m}^{-1}$], the thermal conductivity of the filler particles, is much greater than κ_{m}, the thermal conductivity of the matrix; that is, $\kappa_{\text{f}}/\kappa_{\text{m}} \gg 1$. Physically this means that the flux of heat along a vertical file of particles will be largely confined to the filler and spread significantly into the matrix only near the upper and lower poles of the particles. This means that the thermal conductance G between the polar tangent plane and the cut surface of the hemisphere will be left largely unaffected by:

(i) Mounding highly conductive filler material atop the cut surface, subject to the constraints: (a) the mound be convex; (b) that its volume be rather less than that of the hemisphere; and (c) that its surface be approximately equipotential.
(ii) Adding or subtracting insulating matrix if the regions affected are far from the pole at which the thermal flux through the matrix will be concentrated.

These assumptions enable model construction to proceed along two different paths.

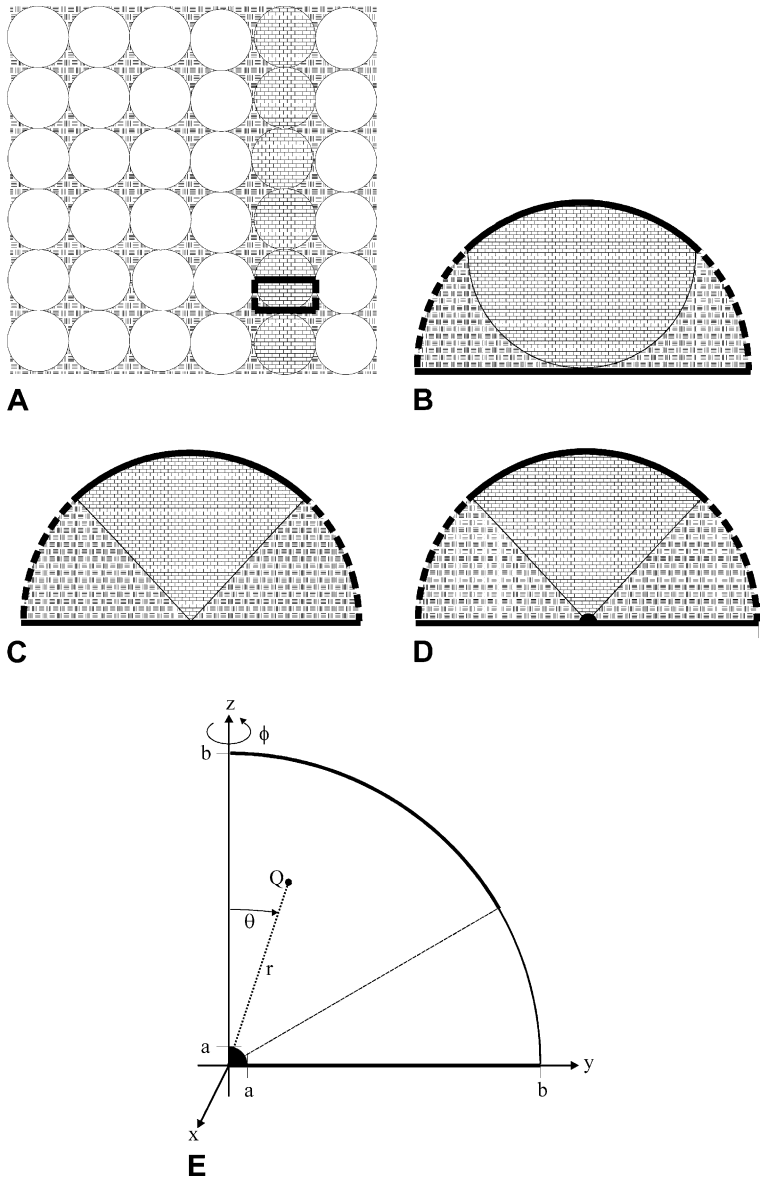

Fig. 1. Derivation of the sphere-cone geometry of Section 3. (A) A simple cubic array of spherical filler particles is shown in yz-cross-section; its extent is infinite in the x- and y-directions and finite but many spheres deep in the z-direction. The stippling indicates a solid matrix within which the spheres are embedded. A typical vertical file of filler particles is indicated by brick fill to denote the presumed crystalline phonon-propagating nature of the particle. The box encloses a single half-cell with isothermal (alternatively, equiflux) top and bottom surfaces (thick black solid lines) and insulating sides (thick black dashed lines). (B) Ontogeny (starting from the half-cell of A) of a half-cell geometry in which Laplace's equation admits of an exact eigenfunction solution. Solid thick black lines denote isothermal (alternatively, equiflux) surfaces; dashed thick black lines denote insulating surfaces. Shown here is the transformation to a hemispherical half-cell with putatively non-perturbing additions of filler and matrix. (C) Transformation of (B) to a half-cell containing a sharp point which would be characteristic of an array of bicones rather than spheres; all interfaces are now simple coordinate boundaries. (D) Putatively non-perturbing transformation of (C) to an analytically tractable geometry; the minute isothermal hemisphere at the origin obviates singularities of the radial eigenfunctions. (E) yz-section through the hemispherical half-cell of (D) showing it divided into two spherical sectors by a cone of angle θ_0. Only one quadrant is shown, and there is ϕ-symmetry about the polar z-axis; the spherical (θ, ϕ, r) coordinate system is illustrated relative to a point Q. The closed spherical sector $0 \leqq \theta \leqq \theta_0$ is symmetrical about its polar axis (zero flux), has constant flux density over its $r = b$ surface, and is at temperature zero over its $r = a$ surface. The open spherical sector $\theta_0 \leqq \theta \leqq \pi/2$ has temperature zero over its $\theta = \pi/2$ surface, zero flux over its $r = b$ surface, and zero temperature over its $r = a$ surface. Boundary conditions on the cone $\theta = \theta_0$ are continuity of temperature and flux.

The first path, shown in Fig. 1B, begins by assuming that the spherical filler particles are s [m] in radius and that the $2s \times 2s \times s$ rectangular–parallelepipedal half-cell has been expanded into an inverted bowl of radius $b = s\sqrt{2}$. In this transformation, high conductivity filler has been added to the top of the hemispherical filler particle increasing its volume by not quite one-third; however, since the thermal resistance will be concentrated near the particle's point of tangency with its lower neighbor, this addition should not materially change the conductance of the half-cell. At the same time, the volume of insulating matrix has been increased by not quite two-thirds, but only far from the point of tangency where is should have no significant effect. However, the problem still is not in an analytically tractable form: that is achieved by approximating the initial filler particle by a cone, as shown in Fig. 1C. Here, all surfaces are simply represented in a (θ, ϕ, r) spherical coordinate system, and Laplace's equation for steady-state heat distribution is separable. Nevertheless, to enable an exact solution in the form of an eigenfunction expansion it is still necessary to add, as in Fig. 1D, a small isothermal (i.e., perfectly-conducting) hemisphere of radius $a \ll b$ around the apex of the cone. This is a mathematical convenience which suppresses a singularity at the origin manifested by the radial eigenfunctions; but it finesses in passing the physical issue of the thermal boundary resistance of a point contact.

The second path, shown in Fig. 2A, begins by shrinking the parallelepiped containing the filler hemisphere to a right circular cylinder of radius s and height s. The filler volume within the half-cell is unchanged; but the matrix volume is decreased, all matrix loss occurring in low flux regions far from the point of tangency at the hemisphere's pole. Laplace's equation is not usefully separable in this (r, θ, z) cylindrical system since the surface separating filler and matrix does not lie along a surface on which one of the coordinates is constant. Since, however, the interface coordinates of the hemisphere can be represented by an equation of the form

$$r = sf(z/s), \tag{2}$$

where $f(z/s)$ increases monotonically from 0 to 1 as z tends from 0 to 1, it follows that a suitable *approximate*

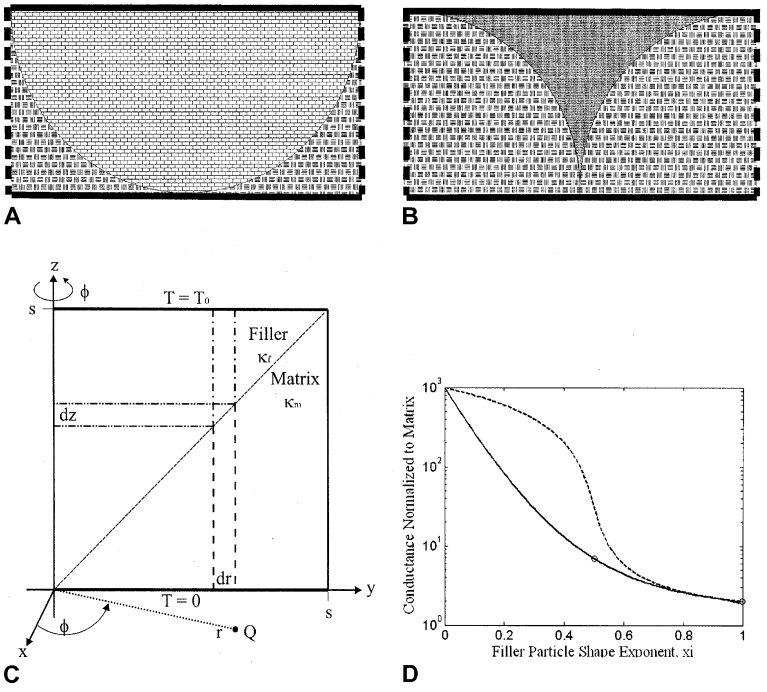

Fig. 2. Transformation of the half-cell of Fig. 1A from a rectangular parallelepiped to a truncated cylinder suitable for *approximate* solution. (A) Solid thick black lines denote isothermal (alternatively, equiflux) surfaces; dashed thick black lines denote insulating surfaces. Shown here is the transformation to a half-cell with a hemispherical filler particle. (B) Topologically equivalent half-cell in which the filler particle has a cusp. (C) The cylindrical half-cell of Fig. 2A and B, here modified to show thin cylindrical shells and a thin cylindrical plate which are used in the approximate theories of Section 4. (D) Approximate solutions for $\mathscr{G}_{\mathrm{norm}}(\xi, \beta)$ for $\beta = (\kappa_f/\kappa_m - 1) = 999$ and $0 < \xi \leqq 1$. The solid line (—) is for the conductances-in-series approximation of Eq. (31), spans the ξ-interval (0.00, 0.99) and at the upper end of this range is beginning to manifest incipient breakdown of the calculation method used for the hypergeometric function; the points denoted by circles (○) are for the special solutions of Eqs. (32) and (33) for $\xi = 1/2$ and 1, respectively. The dashed line (-----) is for the quasi-distributed network model of Eq. (39).

solution method-should work for a wide range of interface shapes which satisfy the monotonicity and range constraints placed upon $f(z/s)$: for example the cusped interface of Fig. 2B.

3. Exact solution for the model of Fig. 1D

3.1. Formal eigenfunction solution

The idealization of Fig. 1D is elaborated in Fig. 1E which illustrates a yz-cut through the geometry and shows the spatial relationships among the several variables. Strictly speaking, the angle θ_0 should be $\pi/4$ as in the half cell of Fig. 1A; but no additional labor ensues solving for an arbitrary $0 < \theta_0 < \pi/2$. The variable of interest is the thermal conductance $\mathscr{G}$ [W/K] between the outer surface of the closed spherical sector of filler and the isothermal $\theta = \pi/2$ plane. However, the underlying problem in the physics of composites concerns the *failure* of the composite's effective conductivity to approach that of the filler; hence a more informative quantity to study would be the behavior of a $\mathscr{G}$ normalized to an appropriate reference conductance, such as that expected of a filler half-cell 2b in diameter and s high, that is $\mathscr{G}/(\pi\sqrt{2}b\kappa_f)$. Nevertheless the conductance will be normalized to a half cell of matrix because that is the tradition in the literature (e.g. [12–15])

$$\mathscr{G}_{\text{norm}} = \mathscr{G}/(\pi\sqrt{2}b\kappa_m). \tag{3}$$

Let $\mathscr{F}$ [$\mathrm{W\,m^{-2}}$] be the normal component of the *inward* thermal flux density, assumed constant over the $r = b$ surface of the filler particle. Then the total inward thermal flux through the hemispherical half-cell of Fig. 1E will be $\mathscr{F}[2\pi b^2(1-\cos\theta_0)]$; and an acceptable normalized conductance is

$$\mathscr{G}_{\text{norm}} = \mathscr{G}/(\pi s\kappa_m) = \sqrt{2}b(1-\cos\theta_0)\frac{\mathscr{F}}{T_0\kappa_m}, \tag{4}$$

where T_0 [K] is the polar temperature (i.e., $T_f(0, \phi, b) = T_f(0, b)$) of the filler particle; this temperature is taken relative to a zero reference over the surface $r = a$ and over the plane $\theta = \pi/2$. This choice of reference temperature may seem a bit unusual since conductances are more commonly computed as the quotient of total thermal flux divided by the temperature of an isothermal surface. However, $\kappa_f/\kappa_m \gg 1$ for the case of interest; and in this limit, $T_f(\theta, b)$ is very close to constant, as will be shown numerically later in this paper. Thus, *physically*, the isothermal and equiflux boundary conditions are virtually indistinguishable; whereas the latter choice greatly simplifies the problem *mathematically*.

The conductance problem has now reduced to finding T_0, which necessitates finding solving the ϕ-independent Laplace equation in both the closed spherical sector of filler and the open spherical sector of matrix and then matching solutions at their interface. This is straightforward classical applied mathematics, but only if one correctly makes a number of decisions which were obvious to the author only a posteriori.

Suppose Laplace's equation in the filler particle is satisfied by

$$T_f(\theta, r) = A_f/r + B_f + \left[\frac{\mathscr{F}b^2}{a\kappa_f}\right]\Phi_f(\theta, r), \tag{5}$$

where A_f and B_f are constants to be determined and

$$\nabla^2 T_f = 0, \tag{6a}$$

$$\kappa_f[\partial T_f/\partial r] = \mathscr{F}, \quad r = b, \tag{6b}$$

$$T_f = 0, \quad r = a, \tag{6c}$$

$$T_f \text{ bounded} \quad \theta = 0. \tag{6d}$$

$$\nabla^2 \Phi_f = 0, \tag{7}$$

$$\partial\Phi_f/\partial r = 0, \quad r = b, \tag{8a}$$

$$\Phi_f = 0, \quad r = a, \tag{8b}$$

It then follows from Eqs. (5) and (6) that

$$A_f = -a\left[\frac{\mathscr{F}b^2}{a\kappa_f}\right], \tag{9a}$$

$$B_f = \left[\frac{\mathscr{F}b^2}{a\kappa_f}\right], \tag{9b}$$

$$T_f = \left[\frac{\mathscr{F}b^2}{a\kappa_f}\right]\{1 - a/r + \Phi_f\}. \tag{10}$$

With the substitution of χ for $\cos\theta$, the Laplace equation for Φ_f can be separated into two ordinary differential equations, one for the radial eigenfunctions $\mathscr{R}_v(r)$ and one for the angular eigenfunctions $\mathfrak{A}_v(\chi)$

$$\frac{\mathrm{d}}{\mathrm{d}r}\left[r^2\frac{\mathrm{d}\mathscr{R}_v}{\mathrm{d}r}\right] - v(v+1)\mathscr{R}_v = 0, \tag{11a}$$

$$\frac{\mathrm{d}}{\mathrm{d}\chi}\left[(1-\chi^2)\frac{\mathrm{d}\mathfrak{A}_v}{\mathrm{d}\chi}\right] + v(v+1)\mathfrak{A}_v = 0, \tag{11b}$$

where, by a well-known theorem of Sturm–Liouville theory (e.g., [16, s. 25], the eigenvalues v $(v+1)$ must be purely real. Moreover, each of the $\mathscr{R}_v$ must satisfy the radial boundary conditions on Φ_f; and each of the $\mathfrak{A}_v$ must be well behaved at $\theta = 0$.

Eq. (11a) for the radial eigenfunctions admits of a solution of the form

$$\mathscr{R}_v(r) = C_v r^v + D_v r^{-(v+1)}, \tag{12}$$

C_v and D_v being constants. By Eqs. (8), these eigenfunctions will be identically zero unless

$$\left[\frac{b}{a}\right]^{(2\nu+1)} = -\frac{\nu+1}{\nu}. \tag{13}$$

To discover the allowed values of ν, let $\nu = \sigma + i\tau$ and apply the condition that the eigenvalues must be real. It then follows that either (i) the eigendegree is purely real or (ii) $\sigma = -1/2$.

If the eigendegree is purely real, then σ must lie in the interval $(-1,0)$ because the left-hand side of Eq. (13) is non-negative. With the substitutions $\Lambda = \ln(\frac{b}{a})$ and $\sigma = -1/2 + 1/2\mu$ it follows that μ lies in the interval $(-1,1)$ and

$$\Lambda = \frac{1}{\mu}\ln\frac{1+\mu}{1-\mu}. \tag{14}$$

The following properties are then readily deduced from Eq. (14): (a) if μ is a root, then so is $-\mu$; (b) $\Lambda(\mu)$ is symmetrical about $\mu = 0$ and has a *minimum* of 2 at $\mu = 0$; (c) because $b/a \gg 1, \Lambda > 2$ and the two roots $+\mu_0$ and $-\mu_0$ give rise to eigendegrees $\nu = -1/2 \pm 1/2\mu_0$ and a zeroeth degree eigenfunction of the form

$${}_0\mathscr{R}_\nu = \left(\frac{r}{a}\right)^{-1/2+1/2\mu_0} - \left(\frac{r}{a}\right)^{-1/2-1/2\mu_0}, \quad k = 0. \tag{15}$$

If the eigendegree is $-1/2 + i\tau$, Eq. (13) implies

$$2\tau = \tan\Lambda\tau. \tag{16}$$

Eq. (16) generates an infinite sequence of eigendegrees with the easily verified properties: (a) the solution for $\tau = 0$ is trivial because Eqs. (8b) and (12) render its radial eigenfunction identically zero; (b) if τ is a solution, then so is $-\tau$; (c) for positive integers k,

$$\tau_k \sim \frac{\pi}{2\Lambda}(2k+1); \tag{17}$$

(d) a suitable radial eigenfunction is

$${}_k\mathscr{R}_\nu = (r/a)^{-\frac{1}{2}}\sin\left(\tau_k \ln\frac{r}{a}\right), \quad k = 1,2,3,\ldots. \tag{18}$$

Eq. (11b) for the angular eigenfunctions is of course Legendre's equation of degree ν and order 0. However, rather than constructing the angular eigenfunctions ${}_k\mathfrak{N}_\nu(\chi)$ from the usual Legendre functions of the first (P_ν) and second (Q_ν) kinds, it is markedly more convenient to note that $P_\nu(\chi)$ and $P_\nu(-\chi)$ are solutions [17, s. 3.2], linearly independent for non-integral ν [17, Eq. 3.4(14)]. Hence, ${}_k\mathfrak{N}_\nu(\chi)$ can legitimately have the form

$${}_k\mathfrak{N}_\nu(\chi) = {}_k\mathscr{G}_\nu P_\nu(\chi) + {}_kH_\nu\overline{P}_\nu(\chi), \tag{19}$$

where $\overline{P}_\nu(\chi) = P_\nu(-\chi)$, ${}_kG_\nu$ and ${}_kH_\nu$ are constants, and $\nu = \nu_k$. However, as $\theta \to 0$ (the polar axis of the filler particle), $\cos\theta \to 1$ and $\overline{P}_\nu(\chi)$ is unbounded; hence ${}_kH_\nu = 0$ and ${}_k\mathfrak{N}_\nu(\chi)$ contains only $P_\nu(\chi)$.

Therefore

$$\Phi_{\mathrm{f}}(\theta,r) = \sum_{k=0}^{\infty} {}_kF_{\nu k}\mathscr{R}_\nu(r)P_\nu(\chi), \tag{20}$$

where the ${}_kF_\nu$ are constants and the subscript ν is an abbreviation for ν_k.

The solution for the temperature in the matrix is similar except that: (a) the radial boundary conditions cause $A_\nu = B_\nu = 0$ while leaving the ν_k unchanged; and (b) the angular boundary condition on the plane $\theta = \pi/2$ produces angular eigenfunctions of the form $P_\nu - \overline{P}_\nu$. Thus

$$\begin{aligned} T_{\mathrm{m}} &= \left[\frac{\mathscr{F}b^2}{a\kappa_{\mathrm{f}}}\right]\Phi_{\mathrm{m}}(\theta,r) \\ &= \left[\frac{\mathscr{F}b^2}{a\kappa_{\mathrm{f}}}\right]\sum_{k=0}^{8} {}_kM_{\nu k}\mathscr{R}_\nu(r)[P_\nu(\chi) - \overline{P}_\nu(\chi)], \end{aligned} \tag{21}$$

the ${}_kM_\nu$ being constants.

To complete the solution for T_{f} requires that the two usual thermal boundary conditions [18, cf. s. 1.9] of (i) continuity of temperature and (ii) continuity of thermal flux be applied over the cone $\theta = \theta_0$:

$$T_{\mathrm{f}}(\chi_0,r) = T_{\mathrm{m}}(\chi_0,r), \quad \chi_0 = \cos\theta_0, \tag{22a}$$

$$\kappa_{\mathrm{f}}\frac{\partial T_{\mathrm{f}}}{\partial\chi} = \kappa_{\mathrm{m}}\frac{\partial T_{\mathrm{m}}}{\partial\chi}, \quad \chi = \chi_0. \tag{22b}$$

Because the ${}_kR_\nu(r)$ constitute a complete orthogonal set on (a, b) [16, s. 24], Eqs. (22) can teased apart to yield two algebraic equations for each value of $k = 0,1,2,\ldots$

$$\mathbf{I}_k/\mathbf{W}_{kk} = {}_kF_\nu[-P_\nu] + {}_kM_\nu[P_\nu - \overline{P}_\nu], \quad \chi = \chi_0, \tag{23a}$$

$$0 = [\kappa_{\mathrm{f}}/\kappa_{\mathrm{m}}]{}_kF_\nu[P'_\nu] + {}_kM_\nu[-P'_\nu - \overline{P}'_\nu], \quad \chi = \chi_0, \tag{23b}$$

where the notation $'$ denotes $\partial/\partial\chi$ and where

$$\mathbf{I}_k = \int_a^b [1 - a/r]_k\mathscr{R}_\nu(r)\,\mathrm{d}r, \tag{24a}$$

$$\mathbf{W}_{kk} = \int_a^b {}_k\mathscr{R}_\nu(r)^2\,\mathrm{d}r. \tag{24b}$$

It then follows from Eqs. (4), (5), (10), (20) and (23) that the normalized conductance of the half-cell is given by

$$\begin{aligned} &\mathscr{G}_{\mathrm{norm}} \\ &= \frac{\sqrt{2}[1-\cos\theta_0]}{1 - \frac{a}{b} + \sum_{k=0}^{\infty}{}_k\mathscr{R}_\nu(b)\frac{\mathbf{I}_k}{\mathbf{W}_{kk}}\frac{P\nu'_\nu - \overline{P}'_\nu}{[\kappa_{\mathrm{f}}/\kappa_{\mathrm{m}}]P'_\nu[P_\nu - \overline{P}_\nu] - P_\nu[P'_\nu - \overline{P}'_\nu]}} \\ &\quad \times \frac{\kappa_{\mathrm{f}}}{\kappa_{\mathrm{m}}}\frac{a}{b}, \quad \chi = \chi_0. \end{aligned} \tag{25}$$

3.2. Computational details

The values of τ_k for the complex eigendegrees can be found by expressing Eq. (17) in the form

$$\tau_k = \frac{\pi}{2\Lambda}(2k+1) - \eta_k, \quad k = 1,2,3,\ldots. \tag{17′}$$

where it turns out that $0 \ll \eta_k \ll 1$. This substitution of Eq. (17′) into Eq. (16) then yields

$$\eta_k = \frac{1}{\Lambda}\arctan\left\{\frac{1}{\frac{\pi}{\Lambda}(2k+1) - 2\eta_k}\right\}. \tag{26}$$

This equation is readily solved by commencing with the approximate solution $\eta_k \sim 1/[\pi(2k+1)]$, plugging it into the right hand side, and iterating to convergence. For example, with $b/a = 1000$, $\eta_1 = 0.103107$ (0.106103, first approximation), $\eta_2 = 0.063080$ (0.063661), $\eta_3 = 0.045268$ (0.045472). In the calculations reported here, 256 terms of the eigendegree series were usually summed; at this level of approximation, the ${}_kF_v$ and the ${}_kM_v$ were less than 10^{-14} and the temperatures on the two sides of the cone were indistinguishable in plots.

Because the integrands of Eqs. (24a) and (24b) are algebraic and simple, $\mathbf{I}_k$ and $\mathbf{W}_{kk}$ are readily expressed and computed.

The functions Legendre functions $P_v(\chi)$ and $\mathsf{P}_v(\chi)$ were expressed by ${}_2\mathrm{F}_1$ hypergeometric functions as follows [17, cf. s. 3.2]:

$$P_v(\chi) = {}_2F_1(-v, 1+v; 1; 1/2 - 1/2\chi), \quad 0 \leqq \chi \leqq 1, \tag{27a}$$

$$\mathsf{P}_v(\chi) = {}_2\mathrm{F}_1(-v, 1+v; 1; 1/2 + 1/2\chi), \quad 0 \leqq \chi \leqq \chi_0 < 1. \tag{27b}$$

These hypergeometric functions are obviously real for real v; and turn out also to be real for $v = -1/2 + i\tau_k$ [17, Eq. 3.14(4)]. If the value of the argument be denoted by ζ and if $\theta_0 \gtrsim 1/4\pi$, the hypergeometric function is readily computed from its Maclaurin series. In particular, for $n^2 \gg \tau_k^2$, the ratio of the $(n+1)$st term to the nth term can be shown to go asymptotically as ζ; that is, the convergence of the hypergeometric series is ultimately driven by its argument, much as with a geometric series. For derivatives of the angular functions, their series can be differentiated term-by-term and the convergence shown to be qualitatively similar.

3.3. Numerical results and commentary

The standard case for computation was taken to be: $\theta_0 = 1/4\pi$; $b/a = 1000$; $\kappa_f/\kappa_m = 1000$. In this case, the $r = b$ surface of the filler particle was isothermal to within 10% as it was: if $\cos\theta_0 = 0.01$; or if $b/a = 10$ or 10000; or if $\kappa_f/\kappa_m = 10$ or 10000. For $\kappa_f/\kappa_m \gtrsim 100$, a strong preponderance of the temperature drop took place within the r-range $(a, 10a)$.

Fig. 3A shows the variation of conductance normalized to the matrix for $\theta_0 = 30°$ (1°)90°, $b/a = 1000$, and $\kappa_f/\kappa_m = 1000$. The normalized conductance of the half-cell is for a 45° cone is 1.99, very nearly twice that of the embedding matrix. That for a 90° cone is 1092 ; that it is not precisely 1000 may be a result of idealizations made to half-cell geometry to enable an "exact" solution of the problem. G_{norm} does not exceed 10% of that expected from filler until $\theta_0 > 89°$; this illustrates the enormous influence that even a minute amount of insulating matrix can have on the half-cell conductance of a point contact. This result also suggests that the obvious strategy of stacking filler flakes (wafers) rather than spheres or cones may not yield the conductance boost envisioned because perfect packing can not be enforced and even tiny wedges of matrix will greatly lower the half-cell conductance.

Fig. 3B shows the variation of conductance normalized to the matrix for $\log_{10}(b/a) = 1.00(0.10)4.00$. This range was selected because, for thermal greases, pastes, and epoxies, filler particles will commonly be less than 50 μm in extent while their nano-asperities which actually make contact (a) presumably are not less than one crystallographic unit cell in extent (∼0.5 nm) and (b) may behave non-classically when less than ∼5 nm in extent [10]. $\mathscr{G}_{\mathrm{norm}}$ is relatively insensitive to variations of $b/a \gtrsim 1000$, presumably because heat conduction has largely been shunted to the matrix near filler-particle-points this small.

Fig. 3C shows the variation of the half cell conductance normalized to the matrix for $\log_{10}(\kappa_f/\kappa_m) = 1.00(0.10)4.00$; this emphasizes how *little* highly conductive filler increases the thermal conductivity of the composite. This range was selected because the matrix is unlikely to be less thermally conductive than low-molecular-weight non-polar amorphous organic solids (∼0.1 $\mathrm{W\,K^{-1}\,m^{-1}}$); and neither is the filler likely to be more conductive than diamond (∼1000 $\mathrm{W\,K^{-1}\,m^{-1}}$).

4. Three approximate solutions

4.1. Introduction

The procedure followed in Section 3 is in spirit complementary to the "applied mathematics school" of two-phase mixture analysis (e.g., [12–15]) which, for some material property of the composite, seeks to find analytic developments which are rigorous, simply computable, and productive of testable numerical predictions. There is also a "pure mathematics school" which treats the mixture problem as one in homogenization of differential operators (e.g., [19]) and then proves results of a general nature on the behaviors and bounds of solutions, but normally does not develop experimentally testable numerical predictions. The literature of these two schools shows very little overlap.

There is, however, a third possibility: that of using the exact results of Section 3 to guide the development of simplistic (but qualitatively informative) models, which are based upon physical insights into the problem and require only introductory calculus for their elaboration. This is the goal of Section 4.

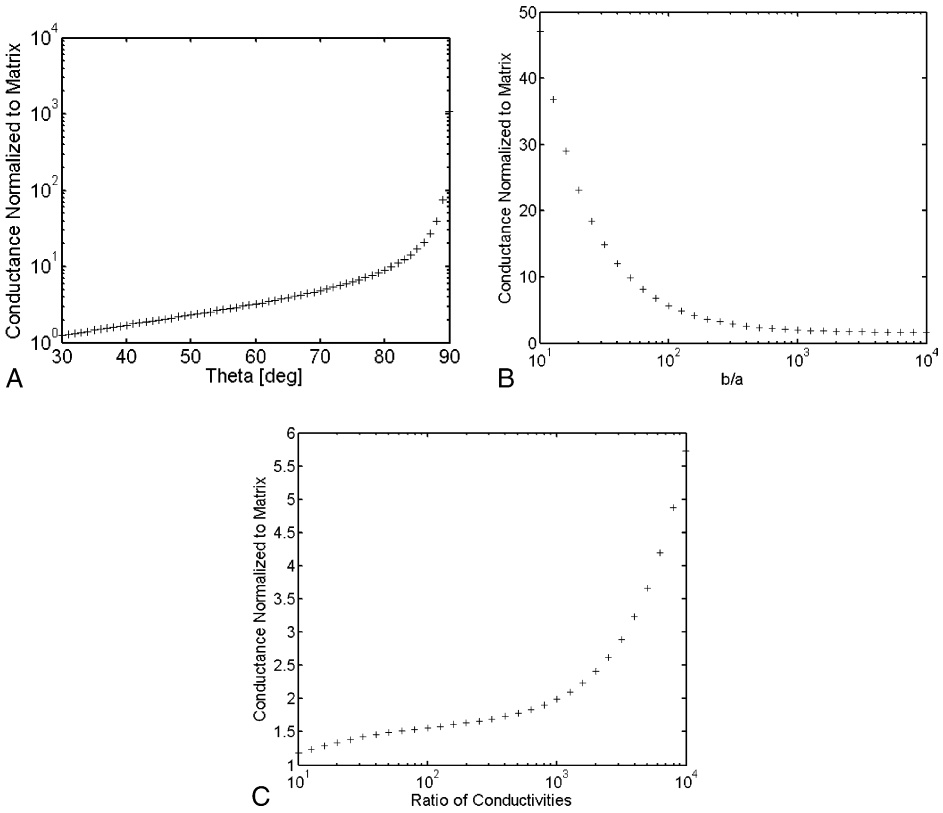

Fig. 3. Numerical results from the sphere–cone geometry of Section 3. (A) Half-cell thermal conductance normalized to matrix, as defined by Eq. (4), versus polar angle θ_0. Parameter values: $b/a = 1000$; $\kappa_f/\kappa_m = 1000$. Observe the enormous reduction in conductance which even a sliver of poorly conducting material can produce. (B) Normalized half cell thermal conductance, as defined by Eq. (4), versus the ratio of bounding radii b/a. Parameter values: $\theta_0 = 45°$; $\kappa_f/\kappa_m = 1000$. Observe that, as b/a becomes large, the normalized conductance seems to stabilize near 2, as if the half-cell was behaving like a circular cylinder of diameter $2b$, height s, and thermal conductivity $2\kappa_m$. (C) Normalized half cell thermal conductance, as defined by Eq. (4), versus the ratio κ_f/κ_m of the thermal conductivities of a filler particle and its suspending matrix. Parameter values: $\theta_0 = 45°$; $b/a = 1000$. Observe that, over the entire range of conductivity ratios employed, the effective conductance of the composite never reaches ten-fold that of the pure matrix.

4.2. A lumped-network conductances-in-series method with numerical results

This model, illustrated in Fig. 2C, contains a thin cylindrical shell of width dr^*, where the $*$ indicates that the variable lies upon a specific surface in the space. The lower portion of this shell, below the dashed (-----) line which denotes the interface $r^*/s = \rho = f(z^*/s) = f(\zeta)$, is denoted by a sparse and heavy dashed line (– – – – –) and is taken to have a top-to-bottom conductance

$$g_m(r^*)dr^* = \frac{\kappa_m(2\pi r^* dr^*)}{z^*}; \tag{28a}$$

it is assumed that $f(1) = 1$. The upper portion of this cell is denoted by a heavy dot-dash line (- · - · - · - · -) and is taken to have a top-to-bottom conductance

$$g_f(r^*)dr^* = \frac{\kappa_f(2\pi r^* dr^*)}{s - z^*}. \tag{28b}$$

Since conductances in series add harmonically, the net top-to-bottom conductance of the shell is

$$g(r^*)dr = (2\pi r^* dr^*)\frac{\kappa_f}{z^*\left(\frac{\kappa_f}{\kappa_m} - 1\right) + s}. \tag{28c}$$

Utilizing the dimensionless variables $\rho = r^*/s$, $\zeta = z^*/s$, $\beta = (\kappa_f/\kappa_m - 1) \gg 1$, and integrating g(r)dr yields [20, Eq. 3.194.5]

$$\begin{aligned}\mathscr{G}_{norm} &= \frac{1}{\pi s \kappa_m}\int_0^s g(r^*)dr^* = 2\xi(\beta+1)\int_0^1 \frac{\zeta^{2\xi-1}d\zeta}{\beta\zeta+1} \\ &= (\beta+1)\,{}_2F_1(1, 2\xi; 1+2\xi; -\beta),\end{aligned} \tag{29}$$

where $f(\zeta)$ has been taken to be ζ^ξ since this power law is capable of mimicking a wide variety of monotonic curves over $(0,1)$; for the physically-realistic concave-upwards cusp-free interface, $0 < \xi \leqq 1$. Eq. (29) can not be evaluated directly by the hypergeometric series;

but it can be transformed by a well-known analytic continuation [17, Eq. 2.1.4(17)] to give

$$\mathscr{G}_{\mathrm{norm}}(\xi,\beta)=\frac{\Gamma(2\xi+1)\Gamma(2\xi-1)}{\Gamma(2\xi)\Gamma(2\xi)}\times\frac{\beta+1}{\beta}{}_2\mathrm{F}_1(1,1-2\xi;2-2\xi;-\beta^{-1})+\frac{\Gamma(2\xi+1)\Gamma(-2\xi+1)}{\Gamma(1)\Gamma(1)}\frac{\beta+1}{\beta^{2\xi}},\quad \xi\neq 1/2,\ \xi\neq 1. \tag{30}$$

Because $\beta^{-1}\ll 1$, this reduces with the aid of the reflection formula to

$$\mathscr{G}_{\mathrm{norm}}(\xi,\beta)=\frac{2\xi}{2\xi-1}\frac{\beta+1}{\beta}[1+\mathscr{O}(\beta^{-1})]+\frac{2\pi\xi}{\sin 2\pi\xi}\frac{\beta+1}{\beta^{2\xi}},\quad \xi\neq 1/2,\ \xi\neq 1; \tag{31}$$

this approximation is plotted in Fig. 2D and reveals that this large β approximation fails above $\xi\sim 0.95$. For $\xi=1/2$, the case of a parabolic contact point and crudely analogous to a sphere, Eq. (29) can be integrated by elementary means to yield

$$\mathscr{G}_{\mathrm{norm}}(1/2,\beta)=\frac{\beta+1}{\beta}\ln(\beta+1); \tag{32}$$

at $\kappa_{\mathrm{f}}/\kappa_{\mathrm{m}}=1000$, this yields 6.915. For $\xi=1$, the case of 45° cone, elementary integration gives

$$\mathscr{G}_{\mathrm{norm}}(1,\beta)=2\frac{\beta+1}{\beta}\left[1-\frac{\ln(\beta+1)}{\beta}\right]; \tag{33}$$

at $\kappa_{\mathrm{f}}/\kappa_{\mathrm{m}}=1000$, this yields 1.988, entirely comparable to the "exact" values from the previous section. For the case $\xi\to 0$, filler fills the entire half-cell, and

$$\mathscr{G}_{\mathrm{norm}}(0,\beta)=\beta+1=\kappa_{\mathrm{f}}/\kappa_{\mathrm{m}}, \tag{34}$$

as would be expected on physical grounds.

4.3. A distributed-network method with numerical results

The geometry of Fig. 2C can also be treated by a rather different approximation. Suppose that the isothermals within the filler particle are planes parallel to the $z=0$ plane. Clearly then, the temperature drop between two such neighboring z-planes will be approximately

$$\mathrm{d}T_{\mathrm{f}}=F_{\mathrm{f}}(\zeta)\frac{\mathrm{d}z}{s^2 f(\zeta)2\pi\kappa_{\mathrm{f}}}, \tag{35a}$$

where $F_{\mathrm{f}}(\zeta)$ is the downward flux of heat, or

$$\frac{\mathrm{d}T_{\mathrm{f}}}{\mathrm{d}\zeta}=F_{\mathrm{f}}(\zeta)\frac{1}{[\pi s\kappa_{\mathrm{f}}]f(\zeta)^2}. \tag{35b}$$

Similarly, the change in $F_{\mathrm{f}}(\zeta)$ due to leakage into the matrix around the perimeter of a plate of thickness $\mathrm{d}z$, must by Eq. (28a), be

$$\frac{\mathrm{d}F_{\mathrm{f}}}{\mathrm{d}\zeta}=T_{\mathrm{f}}(\zeta)[\pi s\kappa_{\mathrm{m}}]\frac{2}{\zeta}f(\zeta)\frac{\mathrm{d}f}{\mathrm{d}\zeta}. \tag{36}$$

If $f(\zeta)$ is once again taken to be ζ^{ξ}, it follows that

$$\zeta^2\frac{\mathrm{d}^2T_{\mathrm{f}}}{\mathrm{d}\zeta^2}+\zeta\frac{\mathrm{d}T_{\mathrm{f}}}{\mathrm{d}\zeta}[2\xi]-T_{\mathrm{f}}\left[\frac{2\xi}{\beta+1}\right]=0. \tag{37}$$

The solution of this equation which matches the boundary conditions $T_{\mathrm{f}}(1)=T_0$ and $T_{\mathrm{f}}(0)=0$ is found by elementary means to be

$$T_{\mathrm{f}}(\zeta)=T_0\zeta^{\gamma}, \tag{38a}$$

$$\gamma=(1/2-\xi)+\sqrt{(1/2-\xi)^2+\frac{2\xi}{\beta+1}}. \tag{38b}$$

It then follows from Eqs. (35b) and (38a) that

$$\mathscr{G}_{\mathrm{norm}}(\xi,\beta)=(\beta+1)\gamma. \tag{39}$$

This is plotted as the dashed line in Fig. 2D. For the 45° cone ($\xi=1$), it matches the prediction of the "exact" solution; and, as $\xi\to 0$ (filler particle fills the half-cell completely), it also agrees with the previous approximation. For $\xi\lesssim 1/2$, the two above approximations clearly differ markedly. Nevertheless, for $\xi\gtrsim 1/2$, they both predict the experimentally familiar and disappointingly small increase in effective conductivity achieved by tightly packing spheres of highly conductive filler [3,4, *e.g.*]. However, for $\xi\gtrsim 0.55$ and $\kappa_{\mathrm{f}}/\kappa_{\mathrm{m}}=1000$, they both predict an increase in effective conductivity less than 10-fold in keeping with the experimental data summarized by Bigg [4, Fig. 7].

4.4. A model which includes the interfacial resistance of the particle's vertex

A high thermal conductivity of particles of a nonmetallic filler depends upon phonon conduction in an ordered crystal lattice. Near filler–matrix interfaces such high conductivity is not expected to be the rule as phonons are scattered (a) by crossing the interface or (b) by surface asperities or other irregularities of structure near the interface. To achieve even a qualitative estimate of these Kapitza-like effects, extensive idealization seems unavoidable.

Suppose then that, as above, the interface shape is described by $r=sf(z/s)$. Further, assume that the phonon-scattering layer can be modelled as a thin film of effective thickness d, within which the effective thermal conductivity is κ_{i}, where $\kappa_{\mathrm{f}}>\kappa_{\mathrm{i}}>\kappa_{\mathrm{m}}$; and let this layer extend into the filler a distance d in the z-direction. It is then possible to proceed in crude analogy with Section 4.2. To this end, assume that:

(i) Within the matrix (cf. Fig. 2C) the field lines are essentially parallel to the z-axis leading to concentric cylindrical shells of end-to-end-resistance

$$R_{\mathrm{m}} = [z^*]/[\kappa_{\mathrm{m}} 2\pi r^* \mathrm{d}r^*]. \tag{40a}$$

(ii) From the interfacial film there arises a resistance contribution

$$R_i = [d]/[\kappa_i 2\pi r^* \mathrm{d}r^*]. \tag{40b}$$

(iii) Within the filler particle the field lines fan out as one might expect, since the apex of the particle should approximate a point source as the conductivity of the matrix becomes very small compared to that of the filler. In particular, suppose that (upon leaving the interfacial film) the field lines fan out conically, starting at (r^*,z^*) in a ring of width $\mathrm{d}r^*$ and ending up at (r,s) in a ring of width $\mathrm{d}r^*[r/r^*]$. It can then be shown that this conical shell of non-uniform thickness has an end-to-end resistance

$$R_{\mathrm{f}} = [s - z^*]/[\kappa_{\mathrm{f}} 2\pi r^* \mathrm{d}r^* (r/r^*)]. \tag{40c}$$

It then follows from the usual substitutions and definition $r/r^* = \mathscr{A}/\rho$ that

$$\begin{aligned}\mathscr{G}_{\mathrm{norm}} &= \frac{1}{\pi s \kappa_{\mathrm{m}}} \int_0^s 2\pi r^* \mathrm{d}r^* \frac{1}{z^*/\kappa_{\mathrm{m}} + \mathrm{d}/\kappa_{\mathrm{i}} + [s - z^*]/[\kappa_{\mathrm{f}}(r/r^*)]} \\ &= 2\int_0^1 \frac{\rho \mathrm{d}\rho}{\zeta + (d/s)(\kappa_{\mathrm{m}}/\kappa_{\mathrm{i}}) + (1-\zeta)(\kappa_{\mathrm{m}}/\kappa_{\mathrm{f}})(\rho/\mathscr{A})}.\end{aligned} \tag{41}$$

This equation reveals that the bulk of the normalized conductance arises from the zone where ζ is very small and terms depending upon $d \ll s$ and possibly $\mathscr{A}/\rho$ predominate. Concerning $\mathscr{A}(\rho)/\rho$ it can reasonably be asserted that (because of fan out) it presumably is large as $\rho \to 0$ and that (because $r \leqslant s$) it tends to unity as $\rho \to 1$. If one assumes moreover that (to keep the field lines from crossing) $\mathscr{A}(\rho)/\rho$ is monotone decreasing over $(0,1)$ and that much of its decrease occurs near $\rho = 0$, then one allowable approximation is

$$\mathscr{A}(\rho)/\rho \doteq \frac{1+\Omega}{1+\Omega\rho^{\omega}}, \tag{42}$$

where ω is rather less than unity and $\Omega \gg 1$. Since $\kappa_{\mathrm{f}} \gg \kappa_{\mathrm{m}}$ and the region near the particle apex dominates, this reduces Eq. (41) to

$$\mathscr{G}_{\mathrm{norm}} \doteq 2\int_0^1 \frac{\rho \,\mathrm{d}\rho}{\zeta + (d/s)(\kappa_{\mathrm{m}}/\kappa_{\mathrm{i}}) + (\kappa_{\mathrm{m}}/\kappa_{\mathrm{f}})\frac{1}{1+\Omega}}. \tag{43}$$

Finally, assuming once more that $\rho = \zeta^{\xi}$ and defining $\zeta_{\min} = (d/s)(\kappa_{\mathrm{m}}/\kappa_i) + (\kappa_{\mathrm{m}}/\kappa_{\mathrm{f}})\frac{1}{1+\Omega}$, yields

$$\mathscr{G}_{\mathrm{norm}} \doteq 2\xi \int_0^1 \frac{\zeta^{2\xi-1}\,\mathrm{d}\zeta}{\zeta + \zeta_{\min}}. \tag{44}$$

As in Section 4.2, this equation can be expressed as a hypergeometric functions. However, given the degree of uncertainty in d, κ_{i}, and Ω, detailed examination of the result seems unwarranted; and this section will conclude by considering only the quasi-parabolic case ($\xi = 1/2$) in the limits $d = 0$ and $\zeta_{\min} \ll 1$. This is

$$\begin{aligned}\mathscr{G}_{\mathrm{norm}} &\doteq \ln(1+\zeta_{min}) - \ln(\zeta_{\min}) \\ &= \ln\left(\frac{1}{\zeta_{\min}}\right) + \zeta_{\min} + \mathscr{O}(\zeta_{\min}^2) \\ &= \ln\left(\frac{\kappa_{\mathrm{f}}}{\kappa_{\mathrm{m}}}\right) + \ln(1+\Omega) + \mathscr{O}(\zeta_{\min}).\end{aligned} \tag{45}$$

4.5. Comparison of the parabolic point contact ($\xi = 1/2$) with the "exact" solution for a simple cubic array of conducting spheres in a less conductive matrix

The solution of Laplace's equation to predict the effective conductivity of a simple cubic array of conducting spheres embedded in a matrix has fascinated applied mathematicians since the time of Lord Rayleigh (cf. [13]). A unified, computable, exact solution has yet to be achieved, although analytic approximations abound. For example:

(i) Batchelor and O'Brien [12] showed that, as $\beta \to \infty$, the normalized conductivity of a closely-packed array of identical spheres varied asymptotically as

$$\frac{\kappa_{\mathrm{eff}}}{\kappa_{\mathrm{m}}} \sim [L\ln(\beta+1) - K], \tag{46}$$

where L and K are constants which vary with the particular type of packing. For example, L is π for a simple cubic array but 4 for a randomly packed array; theoretical values for K were not given. However, in their Fig. 6, Batchelor and O'Brien [Q] fitted Eq. (46) to an extensive set of experimental data for random packing and found (i) that the value of 4 was in good agreement with the data and (ii) that $K \doteq 11$. The authors did not state how large β had to be to make the approximation trustworthy, although McPhedran and McKenzie [14] promptly came up with an estimate of 100.

(ii) For the simple cubic case, Sangani and Acrivos [15] obtained the theoretical result $K = 5.91$. They also extended previous analytic treatments for $\beta \lesssim 50$.

(iii) For the simple cubic case, Cheng and Torquato [13] corrected apparent mistakes in previous analytic treatments for the $\beta \lesssim 50$ regime and extended the method to include simple thermal boundary resistances.

Fig. 4 shows the theoretical curves from Eq. (3.1) of Cheng and Torquato [13] for the small-β regime, from Batchelor and O'Brien [12] for the large-β regime with $L = \pi$ and $K = 5.91$, from Eq. (32) of this paper for the parabolic point contact ($\xi = 1/2$) case of the conductance-in-series approximation, from Eq. (39) of this paper for the parabolic point contact ($\xi = 1/2$) case of

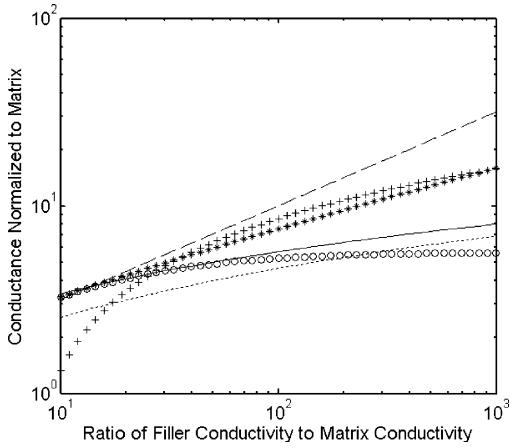

Fig. 4. Comparison of the predicted composite conductances of a simple array of spheres in an insulating matrix; the independent variable is the ratio of filler conductivity to matrix conductivity. The Cheng–Torquato approximation [13] is denoted by a sequence of circles (○ ○ ○ ○ ○ ○); the Batchelor-O'Brien approximation [12] is denoted by a sequence of plus signs (+ + + + + +); the simplistic conductances in series model of Eq. (32) is denoted by a line of small dashes (- - - - - - -); the distributed-network model of Eq. (39) is denoted by a line of coarse dashes (– –); the fan out model of Eq. (45) is denoted by a solid line (—); and finally, the square root heuristic (see text) is denoted by a line of asterisks (* * * * * * *).

the distributed network approximation, and from Eq. (45) of this paper the parabolic point contact ($\xi = 1/2$) case of the fan out approximation with $\Omega = 2$. The obvious conclusion to be drawn from Fig. 4 is that the several models are not in concordance quantitatively even though they all agree qualitatively that greatly increasing the relative thermal conductivity of the filler improves the conductivity of the composite only marginally. Secondarily, of the simplistic approaches of Section 4, it appears that the fan out model is in best accord with the more exact models for cubic arrays.

But finally, as shown by the string of asterisks in Fig. 4, multiplying the distributed network prediction by the fan out prediction and square rooting gives a prediction which tolerably well matches the Cheng–Torquato [13] expansion for values of $\kappa_f/\kappa_m \lesssim 20$ and the Batchelor-O'Brien approximation for values of $\kappa_f/\kappa_m \gtrsim 20$. *Given the non-ideal shapes of filler particles in real physical situations, this "square root heuristic" probably provides as much predictive power as can reasonably be expected; and it is both computationally simple and swift.*

5. Discussion

The literature reviewed in Section 1 showed that the gross oversimplification of Eq. (1c) qualitatively corresponds to experimental reality. The exact and approximate physical models of the previous two sections also substantiate the qualitative validity of Eq. (1c). This does *not* however demonstrate that it is impossible to construct a two-phase heterogeneous paste such that its effective thermal conductivity (or permittivity) is closer to that of the filler than to that of the matrix. Indeed, there are hints in the literature of how one might proceed.

First, in accordance with the predictions of Fig. 2D, one could try to approach the $\xi \to 0$ regime: one could use flake-like filler particles. This has in fact been done (e.g., [1]) and can yield composites with effective conductivity above 25 $\mathrm{W\,m^{-1}\,K^{-1}}$.

Second, reasoning in part that mixtures with higher volume fractions of filler will have higher conductivities, use filler particles whose size distribution is multimodal. At first glance, this might be predicted to be unhelpful for flake fillers, successive layers of which should be in exceptionally close apposition to one another to lower the resistance near contact points; this is so because miscellaneous grit would presumably keep the major flakes from packing tightly. However, electron micrographs of the stacking of quasi-plates reveal that they tend not to settle like bricks in a wall but like bricks dumped in a heap [21, Fig. 15.1]. Therefore, an admixture of sizes might possibly increase the number per unit volume of high conductance contact points with a resultant increase in the effective conductivity of the mixture (cf. [8]). Empirically, the latter possibility seems true [1].

Third, this suggests that for, dimensionally compact (i.e., quasi-spherical) filler particles, it might be advantageous to employ what I shall call *iterative embedding*. Let tiny (e.g., 1 μm) particles of high conductivity κ_f be densely packed into a matrix of much lower conductivity κ_m to obtain a "first composite" of effective conductivity *crudely* estimated by Eq. (45) to be $\kappa_1/\kappa_m \doteq \ln(\frac{\kappa_f}{\kappa m}) + \ln(1+\Omega)$. Into this first composite, densely suspend rather larger filler particles (*e.g.*, 10 μm) to obtain a "second composite" of approximate effective conductivity $\kappa_2/\kappa_1 \doteq \ln(\kappa_f/\kappa_1) + \ln(1+\Omega)$. This process might even be extended one additional level to still larger embedded particles (e.g., 100 μm), and $\kappa_3/\kappa_2 \doteq \ln(\kappa_f/\kappa_2) + \ln(1+\Omega)$. For example, if $\Omega = 2$, $\kappa_m = 1$, and $\kappa_f = 1000$, then $\kappa_1 \doteq 8$, $\kappa_2 \doteq 47$, $\kappa_3 \doteq 197$.

Fourth, however seductive iterative embedding might seem, it should be remembered (A) that uniformly and reproducibly dispersing particles with a sequence of diameter modes will not be trivial and (B) that, long before the result of a sequence of embeddings shall have converged to κ_f, interfacial effects of unknown severity will have vitiated the effectiveness of the process.

6. Conclusions

Loading of a matrix of low thermal conductivity κ_m with uniformly-sized filler particles of much higher thermal conductivity κ_f to obtain a mixture of intermediate

conductivity only slightly less than κ_f seems destined not to work. This is so because the filler's high κ_f is of decisive importance only in minute contact zones between particles; and, near the contact zone, the bulk mechanisms which yielded κ_f may be overwhelmed by Kapitza interfacial-resistance effects. To some extent, it may be possible to avoid this physical limitation by iterative embedding.

Acknowledgment

This paper is dedicated to Professor Fred J. Rosenbaum (1937–1992), whose enthusiasm for the challenges of packaging monolithic microwave integrated circuits first interested the author in this problem.

References

[1] H. Ishida, S. Rimdusit, Very high thermal conductivity obtained by boron nitride-filled polybenzoxazine, Thermochim. Acta 320 (1998) 177–186.
[2] G.K. Batchelor, Transport properties of two-phase materials with random structure, Annu. Rev. Fluid Mech. 6 (1974) 227–255.
[3] D.M. Bigg, Thermally conductive polymer compositions, Polym. Compos. 7 (1986) 125–140.
[4] D.M. Bigg, Thermal conductivity of heterophase polymer compositions, Adv. Polym. Sci. 119 (1995) 1–30.
[5] C. Brosseau, A. Beroual, Computational electromagnetics and the rational design of new dielectric heterostructures, Prog. Mat. Sci. 48 (2003) 373–456.
[6] V.P. Privalko, V.V. Novikov, Model treatments of the heat conductivity of heterogeneous polymers, Adv. Polym. Sci. 119 (1995) 31–77.
[7] E. Tuncer, Y.V. Serdyuk, S.M. Gubanski, Dielectric mixtures: electrical properties and modeling, IEEE Trans. Dielectric Electrical Insul. 9 (2002) 809–828.
[8] L.S. Fletcher, A review of thermal enhancement techniques for electronic systems, IEEE Trans. Components Hybrids Manufact. Technol. 13 (1990) 1012–1021.
[9] E.T. Swartz, R.O. Pohl, Thermal boundary resistance, Rev. Mod. Phys. 61 (1989) 605–668.
[10] D.G. Cahill, W.K. Ford, K.E. Goodson, G.D. Mahan, A. Majumdar, H.J. Maris, R. Merlin, S.R. Phillpot, Nanoscale thermal transport, J. Appl. Phys. 93 (2003) 793–818.
[11] L. Shi, A. Majdumar, Thermal transport mechanisms at nanoscale point contacts, J. Heat Transfer 124 (2002) 329–337.
[12] G.K. Batchelor, R.W. O'Brien, Thermal or electrical conduction through a granular material, Proc. R. Soc. London Ser. A 355 (1977) 313–333.
[13] H. Cheng, S. Torquato, Effective conductivity of periodic arrays of spheres with interfacial resistance, Proc. R. Soc. London Ser. A 453 (1997) 145–161.
[14] R.C. McPhedran, D.R. McKenzie, The conductivity of a lattice of spheres. I. The simple cubic lattice, Proc. R. Soc. London Ser. A 359 (1978) 45–63.
[15] A.S. Sangani, A. Acrivos, The effective conductivity of a periodic array of spheres, Proc. R. Soc. London Ser. A 386 (1983) 263–275.
[16] R.V. Churchill, Fourier series and boundary value problems, McGraw-Hill, New York, 1941.
[17] A. Erdélyi (Ed.), Higher transcendental functions (vol. I), McGraw-Hill, New York, 1953.
[18] H.S. Carslaw, J.C. Jaeger, Conduction of heat in solids, second ed., Oxford, Oxford, 1959.
[19] V.V. Jikov, S.M. Kozlov, O.A. Oleinik, Homogenization of differential operators and integral functions, Springer-Verlag, Berlin, 1994.
[20] I.S. Gradshteyn, I.M. Ryzhik, Table of integrals, series, and products, Academic Press, New York, 1980.
[21] R.M. German, Particle packing characteristics, Metal Powder Industries Federation, Princeton, New Jersey, 1989.